Molecular Catalysis 573 (2025) 114796

Contents lists available at ScienceDirect

Molecular Catalysis

journal homepage: www.journals.elsevier.com/molecular-catalysis

The effect of washing on improving activity of co-precipitated ceria manganese oxide catalysts for volatile organic compound total oxidation

Parag M. Shah, Liam A. Bailey, Zhongyu Jiang, David J. Morgan, Stuart H. Taylor *

Max Planck-Cardiff Centre on the Fundamentals of Heterogeneous Catalysis FUNCAT, Cardiff Catalysis Institute, School of Chemistry, Cardiff University, Translational Research Hub, Maindy Road, Cardiff CF24 4HQ, UK

ARTICLE INFO

Keywords:
Catalytic oxidation
Washing
Ceria
Manganese oxide
VOC

ABSTRACT

Ceria-manganese mixed metal oxide catalysts synthesized by co-precipitation and subsequently washed with varying volumes of hot water were evaluated for effectiveness in the total oxidation of propane and naphthalene. The catalytic activity for both reactions improved with increased washing, with the sample washed with two litres of hot water showing the highest activity. Large differences in the structural and chemical properties were apparent between catalysts, with increased washing producing more crystalline material along with formation of Mn_2O_3 phases. Enhanced washing increased catalyst surface area, decreased concentration of surface contaminants, and increased the concentration of defect oxygen sites, all characteristics known to improve activity for VOC oxidation. This work highlights the need to carefully assess all stages of a catalyst synthesis and identifies washing as an important parameter.

1. Introduction

Volatile organic compounds (VOCs) are a class of common atmospheric pollutants released from anthropogenic and natural emissions, that have a significant negative impact on both the environment and human health [1]. They are typically potent greenhouse gases, with global warming potentials significantly greater than that of carbon dioxide [2], and damaging to human health with increased incidence of cancers like leukaemia linked to exposure to aromatic VOCs [3]. They also readily react with atmospheric NO_x emissions to form low-level ozone and photochemical smog [4]. This is prevalent in urban environments and is a large contributor to air pollution which has been found to significantly damage every organ in the body, and is the primary cause of preventable death worldwide [5]. This has led to the desire to reduce release of VOCs into the atmosphere, with legislation introduced to help encourage limits on emissions [6,7].

Several methods of reducing VOC emissions have been developed, with thermal oxidation, catalytic oxidation, adsorption, and absorption all receiving considerable interest. Catalytic oxidation has proven popular due to destruction of VOCs rather than simply capturing them, whilst compared to thermal oxidation it operates at significantly lower temperatures and it is also more selective towards benign products of carbon dioxide and water, and has the benefit that it is able to successfully treat low concentration streams [8,9].

The total oxidation of propane to carbon dioxide and water has been extensively researched with regards to the control of VOC emissions. The concentration of propane in the atmosphere has increased over the past decade due to increased use of liquified petroleum gas (LPG) as a fuel [10]. It is also a good model reactant to determine catalytic performance for general VOC oxidation due to its high stability, making oxidation particularly challenging [11]. Naphthalene is another VOC that has been extensively studied as it is the simplest poly-aromatic hydrocarbon (PAH), making it a good model reactant for other PAHs [12]. Naphthalene is also highly carcinogenic so controlling emissions is very important.

Traditionally, supported nanoparticles of platinum or palladium have been used as VOC abatement catalysts [13–17]; however, recently there has been an increase in research into metal oxides and mixed metal oxide materials, mainly due to the cheaper cost of these catalysts. Metal oxides of Ce, Mn, Co, Zr, and Fe have all been studied for their effectiveness as a catalyst for the total oxidation of propane [18–27]. Factors such as surface area, metal oxidation state, oxygen lability, and redox potential have all been found to be highly influential on catalyst performance. Previous work by this group has identified ceria-manganese oxide as an effective catalyst for VOC total oxidation [28].

The method by which a catalyst is synthesised is very important. It

* Corresponding author.
E-mail address: taylorsh@cardiff.ac.uk (S.H. Taylor).

https://doi.org/10.1016/j.mcat.2024.114796
Received 12 October 2024; Received in revised form 12 December 2024; Accepted 21 December 2024
Available online 8 January 2025

can significantly influence the factors that drive catalyst activity [29]. It can also affect the introduction of a poison, where choice of precursor or precipitating agent can lead to the formation of known catalyst inhibitors like halogens or sodium at the surface [30,31]. For example, ball milling produced more active catalysts for VOC oxidation compared with precipitation using Na_2CO_3, with one contributing factor being reduced surface Na^+ concentration [18,19]. When synthesising a metal oxide *via* co-precipitation, the sample is often washed to remove soluble impurities, such as residual ions from the precipitating agent. There has been limited investigation into the effect this step has on catalyst performance for VOC oxidation [32]. This study investigates the influence of washing on catalyst physiochemical properties and subsequent effect on activity for propane and naphthalene total oxidation.

2. Experimental

A $Ce_{0.25}Mn_{0.75}O_x$ catalyst was prepared following the method described previously by this group [28]. Materials were made by co-precipitation using an auto-titrator, where an appropriate amount of $Ce(NO_3)_3{\cdot}6H_2O$ (Sigma-Aldrich, Gillingham, UK, 99 %, 0.25 M) and $Mn(NO_3)_2{\cdot}4H_2O$ (Sigma-Aldrich, Gillingham, UK, 99 %, 0.25 M) were added at 3 $mLmin^{-1}$ to a thermostatically controlled water-jacket heated

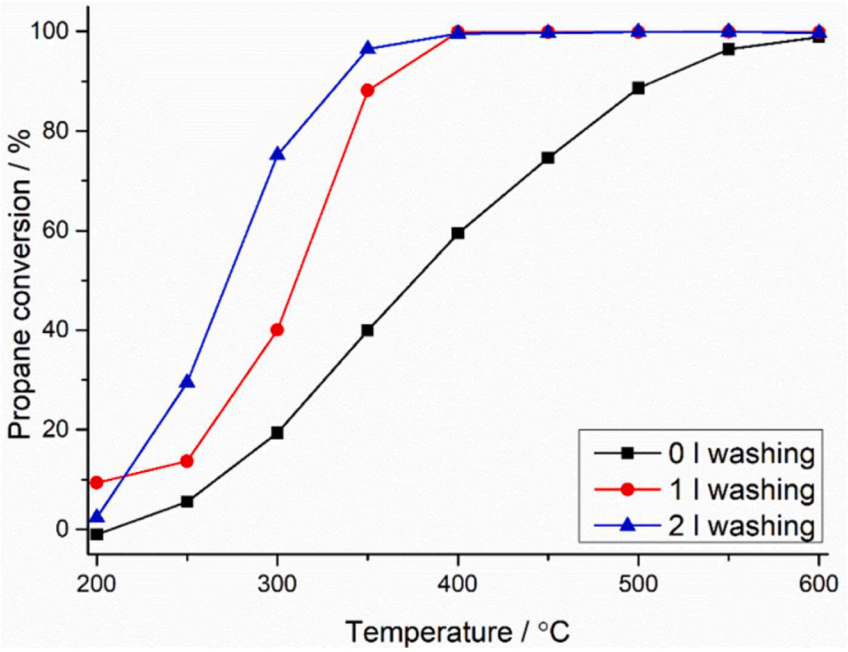

Fig. 1. Propane conversion as a function of temperature for $Ce_{0.25}Mn_{0.75}O_x$ prepared by co-precipitation with sodium carbonate using different washing protocols. Reaction conditions: GHSV = 45,000 h^{-1}, temperature 200–600°C, 5000 ppm propane in air.

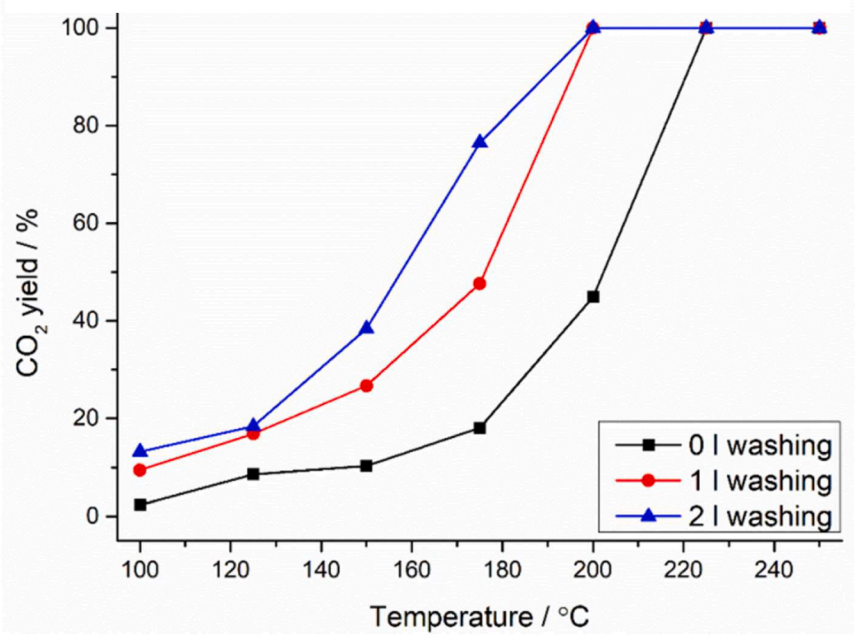

Fig. 2. Catalytic activities for the total oxidation of naphthalene of the $Ce_{0.25}Mn_{0.75}O_x$ prepared via co-precipitation with sodium carbonate using different washing protocols. Reaction conditions: GHSV = 45,000 h^{-1}, temperature 100–250°C, 100 vppm naphthalene in 20 % O_2 balanced with He.

vessel with Na_2CO_3 (1 M) dosed to give a constant pH of 9. The solution was aged at 60°C for 2 h with the precipitate recovered and either left unwashed or washed with either 1 L or 2 L of 90°C deionised water. The sample was then dried at 110°C for 16 h and calcined at 500°C for 3 h under flowing air.

Catalyst activity for the total oxidation of propane was determined using a fixed bed laboratory micro reactor. A reaction feed of 5000 ppm propane in air (BOC, Woking, UK) with a total flow rate of 50 ml min^{-1} was used, with catalysts packed to the same volume, giving a gas hourly space velocity (GHSV) of 45,000 h^{-1}. Analysis was performed using online gas chromatography with flame ionisation and thermal conductivity detectors. Activity was measured between 200 and 600°C with temperature controlled using a k-type thermocouple placed in the catalyst bed. Analysis was performed after steady state activity was achieved with the average of three measurements used at each temperature. Once a measurement had been taken, the furnace temperature was increased and the same procedure repeated. Conversion was calculated from the difference between inlet and outlet concentrations. Conversion data were reproducible to within 2 % and all carbon balances were 100 % ± 5 %. CO_2 was the only reaction product identified.

Catalyst performance for the total oxidation of naphthalene was determined using a separate dedicated fixed bed micro reactor. Naphthalene was sublimed in an isothermal furnace under a flow of He before being mixed with O_2. The gas concentrations used were 100 ppm naphthalene, 10 % O_2 and He balance with a total flow rate of 50 ml min^{-1}. A constant volume of catalyst was used giving a GHSV of 45,000 h^{-1}. Analysis was performed using on line gas chromatography using flame ionisation and thermal conductivity detectors. Activity was measured between 100 −250°C with the temperature controlled by a k-type thermocouple in the catalyst bed. Activity was calculated once steady state had been reached with an average of three measurements used. Activity was expressed as % CO_2 yield, in procedures previously established [33].

Fourier transform infrared (FTIR) spectroscopic analysis was conducted on a Bruker Tensor 27 instrument (Bruker, Derby, UK). Spectra were obtained with 32 scans per spectrum using a resolution of 4 cm^{-1}.

Powder X-ray diffraction (XRD) was conducted on a Panalytical X'Pert instrument (Malvern Panalytical, Malvern, UK) using a Cu X-ray source at 40 kV and 40 mA. Identification of phases was assisted using the ICDD database by matching experimental patterns to standards. The Scherrer equation was used to estimate crystallite size, based on the analysis of line widths of 4 diffraction peaks compared to a silicon standard.

Surface area analysis was performed using a Quantachrome Quadrasorb Evo Analyser (Quantachrome, Hook, UK). Materials were outgassed under vacuum at 120°C for 16 h before a N_2 multipoint adsorption isotherm was measured at −196°C. The Braunauer-Emmet-Teller (BET) method was applied to determine surface area.

Temperature programmed reduction (TPR) was performed on a Quantachrome ChemBET (Quantachrome, Hook, UK) apparatus. Samples were treated under helium for an hour at 120°C before a reduction profile was recorded from room temperature to 900°C under a flow of 10 % H_2/Ar at a flow rate of 50 ml min^{-1}. A ramp rate of 15°C min^{-1} was used.

Scanning electron microscopy (SEM) and electron dispersive X-ray spectroscopy (EDX) were conducted on a Tescan MAIA3 FEG-SEM microscope (Tescan, Cambridge, UK) with an Oxford Instruments X-ray Max^N 80 (Oxford Instruments, Abingdon, UK) detector with samples mounted uncoated on carbon Leit discs. A beam voltage of 15 k V and current of 30 pA were used.

X-ray photoelectron spectroscopy (XPS) was performed using a Thermo Scientific K-Alpha+ (Thermo Fisher Scientific, East Grinsted, UK) using an Al Kα monochromator at 72 W. High resolution and survey scans were recorded with pass energies of 40 and 150 eV, and step sizes of 0.1 and 1 eV respectively. Combined Ar ions and low energy electron fluxes were used to neutralise surface charging. The C (1 s) peak at 284.8 eV was used to calibrate each spectrum. Data analysis was performed on CasaXPS software v2.3.24, removing the Shirley background and applying Schofield sensitivity factors and an energy dependence of −0.6.

3. Results and discussion

The impact of washing on catalyst performance was studied for the total oxidation of both propane and naphthalene. For propane total oxidation, there was negligible activity when using an empty reactor tube (6 % at 600°C) showing that reactions from homogeneous gas phase reactions were minimal. For all catalysts, selectivity towards CO_2 was >99 %, showing that total oxidation to CO_2 and H_2O occurred. Fig. 1 shows the catalyst performance for total propane oxidation. There was an increase in activity as the volume of water used for the washing step increased. The unwashed catalyst performed the worst of all tested, propane conversion increased with temperature, with full conversion achieved at 600°C. When 1 L of water was used to wash the catalyst, a significant increase of activity was accomplished. The temperature at which full propane conversion was achieved was 200°C lower at 400°C. Improved performance was observed when the volume of water used for washing was increased to 2 L. Whilst full propane conversion was recorded also at 400°C, there was a large increase in activity at lower temperature. This is particularly evident at 300°C, where the 2 L sample converted 75 % of the propane, whilst the 1 L catalyst only had 40 % conversion. This clearly demonstrates that washing has a large influence on the activity for propane total oxidation. This is made apparent when comparing the T_{50}s of the materials synthesised (Table 1) along with the rates of reaction. The T_{50} for the sample washed with 2 L was 115 and

Table 1
Activity data for the $Ce_{0.25}Mn_{0.75}O_x$ catalysts prepared via co-precipitation with sodium carbonate using different washing protocols. T_{50} = temperature at which 50 % conversion was achieved. Reaction conditions for propane oxidation: GHSV = 45,000 h^{-1}, temperature 200–600°C, 5000 ppm propane/Air. Reaction conditions for naphthalene oxidation: GHSV = 45,000 h^{-1}, temperature 100–250°C, 100 vppm naphthalene in 20 % O_2 balanced with He.

Catalyst	T_{50} for propane conversion (°C)[a] (error ±2.1°C)	Rate of propane conversion at 300°C (mol s^{-1})[b]	T_{50} for CO_2 yield from naphthalene oxidation[c] (error ± 2.4°C)	CO_2 formation rate from naphthalene oxidation at 175°C (mol s^{-1})[d]
No washing	381	1.67×10^{-5}	203	2.77×10^{-6}
1 L	310	3.61×10^{-5}	176	8.33×10^{-6}
2 L	266	6.94×10^{-5}	158	1.38×10^{-5}

The same trend was also seen for the total oxidation of naphthalene (Fig. 2). Activity increased with more washing with the 2 L being the most active, followed by the 1 L, and the unwashed catalyst being the least active. For the unwashed sample, 100 % CO_2 yield, and hence full conversion of the naphthalene, was obtained at 225°C, whilst both the washed samples reach this conversion at 200°C. The catalyst washed with 2 L had the best lower temperature activity, with a T_{50} of 158°C, lower than the temperature of 176°C for the 1 L washed catalyst, demonstrating that while washing does have an effect on catalyst activity for naphthalene oxidation it was not as influential as it was for propane total oxidation.

[a] calculated error ± 2.1°C.
[b] calculated error for reaction rate ±2. %
[c] calculated error ± 2.4°C.
[d] calculated error for reaction rate ± 3 %.

44°C lower than the unwashed and 1 L catalysts respectively while the rate of propane conversion at 300°C was almost double that of the next best performing catalyst.

Catalyst stability testing was also probed with 72 h time on line performed for each sample at 300°C for propane total oxidation (Figure S1). Minimal decrease in performance was noted over this time period, suggesting that while the amount of washing influences activity, it does not affect catalyst stability.

In order to understand the influence of washing on the catalyst precursor prior to calcination characterisation of the precursor was performed. FTIR analysis (Figure S2) showed the formation of a metal carbonate confirmed by bands centred at 860 and 1400 cm^{-1}. The absence of bands between 3200–3500 cm^{-1} indicated that only a metal carbonate has formed and not a mixed carbonate/hydroxide precursor. Powder XRD patterns (Figure S3) also suggest the formation of a metal carbonate, with peaks associated with both cerium carbonate and manganese carbonate identified, and are broadly similar regardless of the amount of washing performed [34,35]. Surface area analysis (Table S1) showed significant differences between the precursors, with surface area increasing with increased washing. This suggests there are differences in the materials brought about by washing only, that can potentially influence catalyst performance.

X-Ray diffraction analysis of the calcined materials showed significant differences in the diffraction patterns (Fig. 3), showing that washing had a significant impact on the bulk structure of the catalysts formed. In all cases peaks occurred at 28°, 33°, 49°, and 57° corresponding to the (111), (200), (220), and (311) lattice planes of cubic fluorite phase ceria. Additional peaks appeared at 24°, 32°, 39°, 44°, and 52° which relate to the formation of (211), (222), (400), Mn_2O_3 phases. While the manganese phase are present in all samples, they become more well defined with increased washing. This observation can help explain the activity for VOC total oxidation. Mn_2O_3 is a manganese phase recognised as highly active for the total oxidation of both propane and naphthalene, with previous studies showing it to be more active than ceria [28]. Table 2 demonstrates a decrease in the crystallite size with increased washing. This has been seen in other studies into ceria-based mixed metal oxides and is indicative of incorporation of the manganese into the ceria lattice [18–20,28,36,37]. This incorporation has led to an increase in activity for other catalysts studied previously in the literature. The differences in the size of the unit cell also suggest differences in the extent of incorporation of the manganese into the cerium lattice. Incorporation of a smaller atom into the lattice will often see a contraction in the size of the unit cell volume, which can be seen for all catalysts. A unit cell volume of 126.5 $Å^3$ for the unwashed catalyst is smaller than the washed catalysts suggesting that washing is facilitating the removal of the manganese from the cerium lattice, forming the Mn_2O_3 phases.

XRD analysis suggests that both a mixed Ce-Mn phase and Mn_2O_3 phase are present in all catalysts, however, it appears that washing impacts the material structure through the formation of greater amounts of Mn_2O_3. This suggests that the quantity of Mn_2O_3 influences catalyst performance. Previous work by the group [28], has shown that pure Mn_2O_3 is less active than $Ce_{0.25}Mn_{0.75}O_x$. This could suggest that there is synergy between the two phases leading to the improved performance.

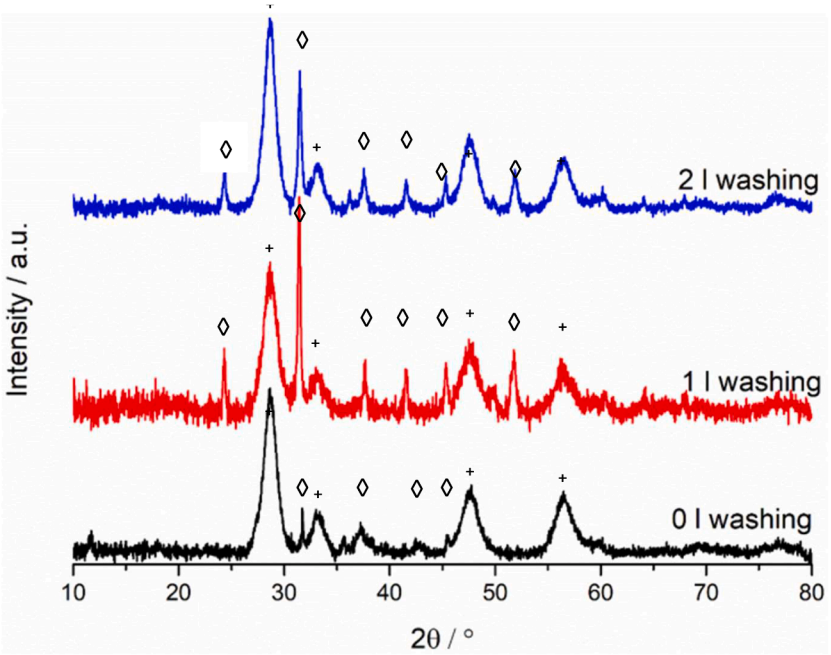

Fig. 3. Powder XRD patterns of the $Ce_{0.25}Mn_{0.75}O_x$ prepared using via coprecipitation with sodium carbonate using different washing protocols. ◊: Mn_2O_3–JCPDS: 089–4836. *: CeO_2–JCPDS: 43–1002.

Table 2
Physicochemical properties and resulting activity data for $Ce_{0.25}Mn_{0.75}O_x$ prepared by coprecipitation with sodium carbonate using different washing protocols determined from XRD and BET data.

Catalyst	Average crystallite size of CeO_2 (Å)	Average Mn_2O_3 crystallite size (Å)	d-spacing of (200) lattice plane (Å)	Unit cell volume ($Å^3$)	Surface area (m^2 g^{-1})	Rate of propane conversion per m^2 at 300°C (mol^{-1} s^{-1} m^{-2})	Rate of CO_2 formation per m^2 at 175°C (mol^{-1} s^{-1} m^{-2})
No washing	65	90	2.51	126.5	32	5.22×10^{-7}	8.66×10^{-8}
1 L	41	152	2.69	155.7	41	8.80×10^{-7}	2.03×10^{-7}
2 L	32	269	2.70	157.5	59	1.18×10^{-6}	2.34×10^{-7}

Surface area analysis was performed on the catalysts (Table 2). Surface area increased with increased washing, again identifying that the washing step is not just removing sodium from the material but also causing changes in the greater structure of the catalysts. As XRD identified the catalysts all have the same crystalline phases present, it is possible to normalise catalyst activity to the surface area, seen in Table 2. Here it is evident that the rate of reaction increases with surface area, demonstrating that the increased surface area due to the washing has a benefit on catalyst performance. Increased surface area has also been shown to be an important parameter to increase catalyst activity for other ceria-based catalysts [18,19,28].

Reduction profiles for the catalysts were measured *via* TPR (Fig. 4), and again showed large differences in the reducibility of the materials formed. The unwashed catalyst has 3 peaks, a broader peak centred at 310°C, and two sharper peaks at 405 and 475°C corresponding to the reduction of MnO_2 to Mn_2O_3, Mn_2O_3 to Mn_3O_4, and Mn_3O_4 to MnO respectively [38]. This identifies the presence of an MnO_2 phase that was not visible in the XRD pattern. This could either be that the amount of MnO_2 is too low to be detected by XRD or that the MnO_2 is present in a more amorphous phase. Both the 1 and 2 L catalysts had 2 major reduction peaks at 290 and 420°C, and 260 and 390°C respectively, corresponding to the reduction of Mn_2O_3 to Mn_3O_4, and Mn_3O_4 to MnO. There is a slight shoulder on the first peak suggesting there may be a small amount of MnO_2 present in these catalysts With increased washing the position of the peaks shifted to much lower temperatures. This would make the catalysts that had been washed to a greater extent more reducible which could lead to a greater amount of active oxygen being present at lower temperature that are available to effect oxidation. These types of catalysts are known to proceed via the Mars van Krevelen reaction mechanism [39], which relies on the active oxygen in the lattice being available to react. Previous studies for VOC oxidation by metal oxides have identified lower temperatures of reduction as being beneficial [21,24,40–42].

Catalyst morphology was probed using Scanning Electron Microscopy (Figure S4). All samples displayed similar bulbous shaped morphologies seen previously for cerium-manganese mixed metal oxides with high manganese concentrations [28]. The micrographs collected from the backscattered electrons showed little contrast for the unwashed catalyst, suggesting good mixing of the cerium and manganese. However, there are areas of contrast apparent in the backscattered electron images of the washed catalysts suggesting that the washing encourages some phase separation of the ceria and manganese oxide species. This corresponds well to the XRD patterns produced where significant diffraction was seen for both ceria and manganese oxide phases.

Elemental analysis by EDX showed differences in the amount of sodium present based on the level of washing (Table 3). The sodium present remains from the sodium carbonate precipitating agent and its presence in high concentrations has been linked to lower catalyst performance in oxidation reactions [43–45]. Both the unwashed and 1 L sample had around 5 atomic % concentration of sodium present, much higher than the 0.6 atomic% seen for the 2 L washed catalyst. This shows that it takes a large amount of washing to remove possible reaction inhibitors, and this is an important point to be considered during preparation by precipitation. Previous studies into the effects of residual sodium have shown that it can inhibit catalyst reducibility leading to reduced activity for VOC oxidation [32,46]. This has been seen in the materials tested here where reduction of the catalysts proceeds at lower temperatures the more it is washed. EDX also shows that the bulk

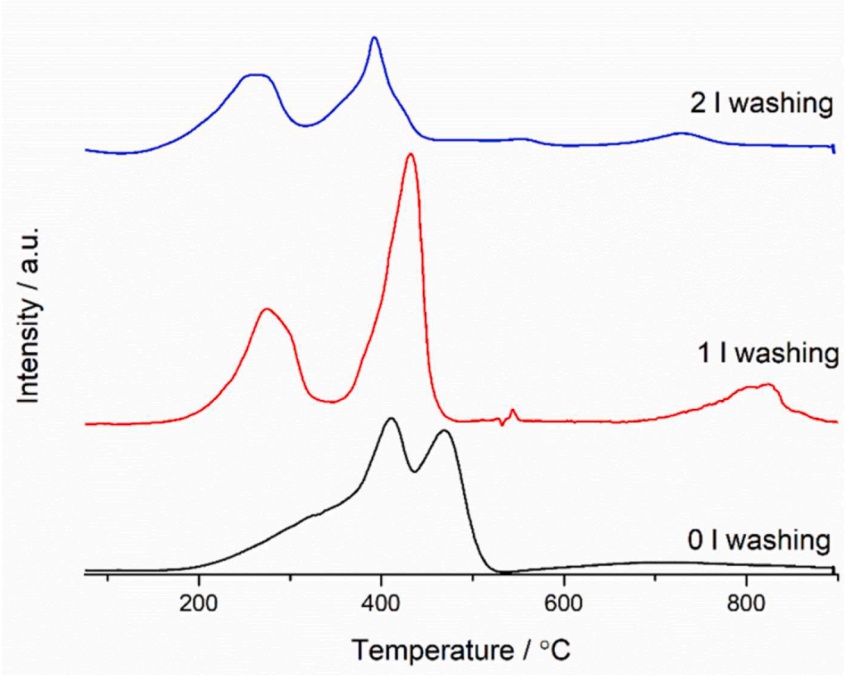

Fig. 4. Hydrogen temperature programmed reduction profiles of the $Ce_{0.25}Mn_{0.75}O_x$ prepared via coprecipitation using different washing protocols.

Table 3
Elemental composition of the synthesised catalysts derived from EDX and XPS data.

Catalyst	Concentration (atomic %) derived from EDX analysis				Concentration (atomic %) derived from XPS analysis			
	Ce	Mn	O	Na	Ce	Mn	O	Na
No washing	7.2	22.7	65.2	4.9	14.3	20.3	54.4	15.9
1 L washing	5.1	22.8	66.8	5.3	9.2	15.9	63.0	11.9
2 L washing	5.0	19.6	74.8	0.6	12.4	16.8	70.0	0.8

concentrations of the other elements varies with washing. Any washing leads to a small decrease in the concentration of cerium present in the sample, possibly due to washing away unprecipitated precursor. There is also an increase in the oxygen concentration with washing. Elemental mapping was also performed during the EDX analysis (Figure S5) showing large amounts of separation between the ceria and manganese oxide phases, correlating well with the XRD and SEM analysis.

X-ray photoelectron spectroscopy was performed to establish surface elemental composition of the catalysts (Table 3). The results are consistent with the EDX results, where increased washing led to a decrease in the amount of sodium present. Surface sodium has been shown to inhibit catalyst activity for reasons including blocking access to active sites, reducing oxygen mobility and encouraging alternative reaction pathways [46]. This again supports the idea that the amount of sodium present inhibits catalyst activity and that increased washing is able to remove Na^+ and hence improve activity. There is also a large difference in the concentrations of sodium observed when comparing the EDX and XPS, with the XPS values being much higher. It suggests much higher concentrations remain at the catalyst surface compared to the bulk, this again highlights the importance of washing of these catalysts. Comparison between the sodium elemental analysis determined by EDX and XPS is also interesting as it appears to show differences in the mechanism of how the Na is removed by washing. After 1 L of washing, EDX shows no change in the relative Na concentration present, while XPS showed a decrease from 15.9 atomic % to 11.9 atomic %. This suggests that sodium is removed from the surface first before being removed from the bulk.

Further XPS analysis of the Ce 3d and Mn 2p regions are presented in Fig. 5. In all cases, the catalysts showed very similar surface chemical states for the ceria and manganese, with washing having negligible effect. For the ceria, a large amount was present as Ce^{4+} due to the large peak centred at 917 eV, whilst the symmetry of the peaks at 881 and 889 eV indicated that the Ce^{3+} was also present. The level of symmetry did not change with washing suggesting that the proportion of Ce^{3+} present was consistent regardless of the amount of washing performed. The Mn 2p spectra also suggests that the chemical state of the manganese was similar due to the shape and position of the peaks present.

The O 1 s spectra are presented in Fig. 6, detailing the presence of lattice oxygen species (O_α) and defect oxygen species (O_β). The presence

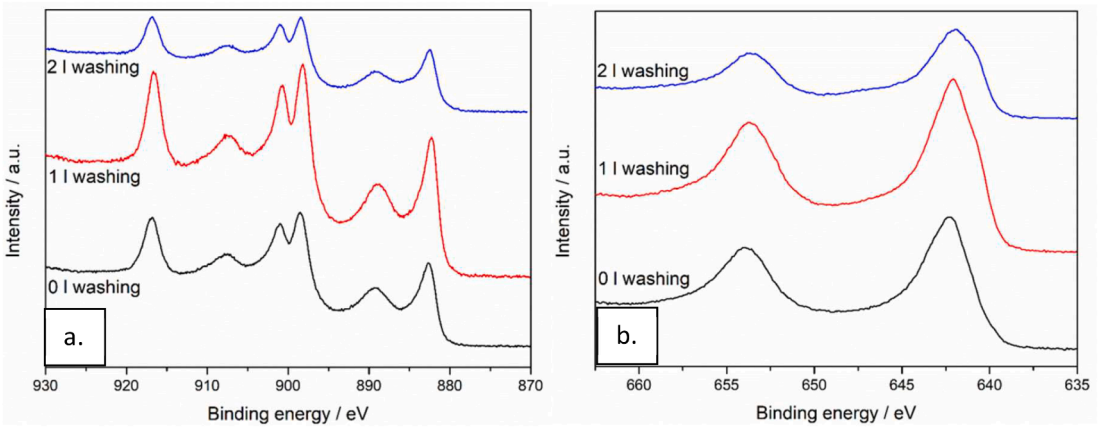

Fig. 5. XPS spectra of the for the $Ce_{0.25}Mn_{0.75}O_x$ prepared using different washing protocols. A. Ce 3d B. Mn 2p.

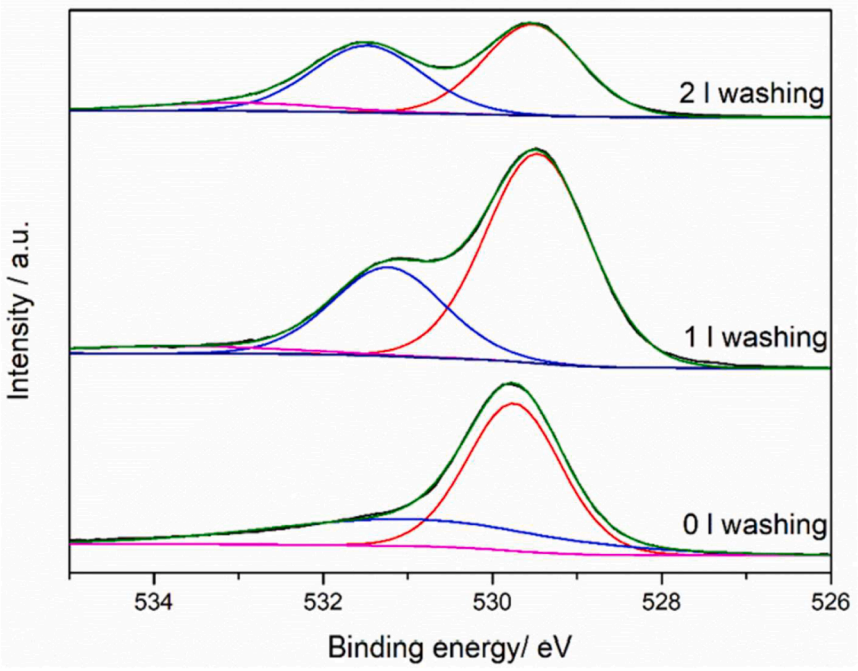

Fig. 6. XPS spectra for the O 1 s peak the $Ce_{0.25}Mn_{0.75}O_x$ prepared via coprecipitation using different washing protocols.

Table 4
XPS derived concentrations of the lattice and defect oxygen species for the $Ce_{0.25}Mn_{0.75}O_x$ prepared using different washing protocols.

Catalyst	Relative concentration of O_α (%)	Relative concentration of O_β (%)
No washing	74.4	15.6
1 L washing	68.7	31.3
2 L washing	50.2	49.8

and concentration of defect sites have been linked to increased activity for VOC oxidation in many studies [47–49]. All catalysts had these defect oxygen sites, with the relative proportion compared to the lattice oxygen species, increasing with increased washing, which is demonstrated in Table 4. This is another factor that can help to explain the relationship between activity and washing as the increased density of highly active defect oxygen sites promotes greater VOC conversion [50–52]. Defect engineering has been a prominent topic of research over the past few years, so washing could provide a simple way of increasing their concentration.

4. Conclusions

$Ce_{0.25}Mn_{0.75}O_x$ mixed metal oxide catalysts were prepared *via* co-precipitation with sodium carbonate and were either unwashed or washed with 1 L or 2 L of hot water during the synthesis. While all catalysts were active for the total oxidation of both propane and naphthalene, activity increased for both reactions with the volume of water used for washing. Washing leads to changes in the structure of the catalyst, evidence through analysis of the washed precursor, that is maintained after calcination. Washing enables the removal of manganese from the ceria lattice forming highly active Mn_2O_3 phases, which appear to work synergistically with the remaining mixed Ce-Mn phases to successfully oxidise VOCs. Characterisation also showed significant differences in the physical and chemical properties of the catalysts with improved performance also ascribed to increased surface area, lower surface Na^+ concentration, and higher concentration of defect oxygen sites that occurred with additional washing. This work shows that every step of a catalyst synthesis is highly influential and that small changes can lead to large differences in catalyst characteristics and subsequent activity.

CRediT authorship contribution statement

Parag M. Shah: Writing – review & editing, Investigation, Formal analysis. **Liam A. Bailey:** Writing – original draft, Formal analysis. **Zhongyu Jiang:** Writing – review & editing, Formal analysis, Investigation. **David J. Morgan:** Writing – review & editing, Formal analysis. **Stuart H. Taylor:** Writing – review & editing, Supervision, Funding acquisition, Conceptualization.

Declaration of competing interest

The authors declare that they have no known competing financial interests or personal relationships that could have appeared to influence the work reported in this paper.

Acknowledgements

XPS data collection was performed at the EPSRC National Facility for XPS (“HarwellXPS”), operated by Cardiff University and UCL, under contract no. PR16195. The authors would like to thank the CCI-Electron Microscopy Facility which has been part-funded by the European Regional Development Fund through the Welsh Government and The Wolfson Foundation.

Supplementary materials

Supplementary material associated with this article can be found, in the online version, at doi:10.1016/j.mcat.2024.114796.

Data availability

Data will be made available upon request.

References

[1] C. He, J. Cheng, X. Zhang, M. Douthwaite, S. Pattisson, Z. Hao, Recent Advances in the Catalytic Oxidation of Volatile Organic Compounds: A Review Based on Pollutant Sorts and Sources, Chem. Rev. 119 (7) (2019) 4471–4568, https://doi.org/10.1021/acs.chemrev.8b00408.
[2] M.S. Kamal, S.A. Razzak, M.M. Hossain, Catalytic Oxidation of Volatile Organic Compounds (VOCs) – A Review, Atmos. Environ. 140 (2016) 117–134, https://doi.org/10.1016/j.atmosenv.2016.05.031.
[3] R. Snyder, Leukemia and Benzene, Int. J. Environ. Res. Public Health 9 (8) (2012) 2875–2893, https://doi.org/10.3390/ijerph9082875.
[4] Y. Guo, M. Wen, G. Li, T. An, Recent Advances in VOC Elimination by Catalytic Oxidation Technology onto Various Nanoparticles Catalysts: A Critical Review, Appl. Catal. B Environ. 281 (2021) 119447, https://doi.org/10.1016/j.apcatb.2020.119447.
[5] P.J. Landrigan, R. Fuller, N.J.R. Acosta, O. Adeyi, R. Arnold, N. Basu, A.B. Baldé, R. Bertollini, S. Bose-O'Reilly, J.I. Boufford, P.N. Breysse, T. Chiles, C. Mahidol, A. M. Coll-Seck, M.L. Cropper, J. Fobil, V. Fuster, M. Greenstone, A. Haines, D. Hanrahan, D. Hunter, M. Khare, A. Krupnick, B. Lanphear, B. Lohani, K. Martin, K.V. Mathiasen, M.A. McTeer, C.J.L. Murray, J.D. Ndahimananjara, F. Perera, J. Potočnik, A.S. Preker, J. Ramesh, J. Rockström, C. Salinas, L.D. Samson, K. Sandilya, P.D. Sly, K.R. Smith, A. Steiner, R.B. Stewart, W.A. Suk, O.C.P. van Schayck, G.N. Yadama, K. Yumkella, M. Zhong, The Lancet Commission on Pollution and Health, The Lancet 391 (10119) (2018) 462–512, https://doi.org/10.1016/S0140-6736(17)32345-0.
[6] S. Scirè, L.F. Liotta, F. Supported Gold Catalysts for the Total Oxidation of Volatile Organic Compounds, Appl. Catal. B Environ. 125 (2012) 222–246, https://doi.org/10.1016/j.apcatb.2012.05.047.
[7] M.V. Twigg, Progress and Future Challenges in Controlling Automotive Exhaust Gas Emissions, Appl. Catal. B Environ. 70 (1) (2007) 2–15, https://doi.org/10.1016/j.apcatb.2006.02.029.
[8] A. Krishnamurthy, B. Adebayo, T. Gelles, A. Rownaghi, F. Rezaei, Abatement of Gaseous Volatile Organic Compounds: A Process Perspective, Catal. Today 350 (2020) 100–119, https://doi.org/10.1016/j.cattod.2019.05.069.
[9] M.N. Taylor, W. Zhou, T. Garcia, B. Solsona, A.F. Carley, C.J. Kiely, S.H. Taylor, Synergy between Tungsten and Palladium Supported on Titania for the Catalytic Total Oxidation of Propane, J. Catal. 285 (1) (2012) 103–114, https://doi.org/10.1016/j.jcat.2011.09.019.
[10] G.C. Toon, J.-F.L. Blavier, K. Sung, K. Yu, Spectrometric Measurements of Atmospheric Propane (C_3H_8), Atmos. Chem. and Phys. 21 (13) (2021) 10727–10743, https://doi.org/10.5194/acp-21-10727-2021.
[11] B.A. Tichenor, M.A. Palazzolo, Destruction of Volatile Organic Compounds via Catalytic Incineration, Environ. Prog. 6 (3) (1987) 172–176, https://doi.org/10.1002/ep.670060328.
[12] K. Aggett, T.E. Davies, D.J. Morgan, D. Hewes, S.H. Taylor, The Influence of Precursor on the Preparation of CeO2 Catalysts for the Total Oxidation of the Volatile Organic Compound Propane, Catalysts 11 (12) (2021) 1461, https://doi.org/10.3390/catal11121461.
[13] M. Taylor, E.N. Ndifor, T. Garcia, B. Solsona, A.F. Carley, S.H. Taylor, Deep Oxidation of Propane Using Palladium–Titania Catalysts Modified by Niobium, Appl. Catal. A Gen. 350 (1) (2008) 63–70, https://doi.org/10.1016/j.apcata.2008.07.045.
[14] L.A. Bailey, M. Douthwaite, T.E. Davies, D.J. Morgan, S.H. Taylor, Controlling Palladium Particle Size and Dispersion as a Function of Loading by Chemical Vapour Impregnation: An Investigation Using Propane Total Oxidation as a Model Reaction, Catal. Sci. Technol. 14 (17) (2024) 5045–5053, https://doi.org/10.1039/D4CY00665H.
[15] M.V. Twigg, Catalytic Control of Emissions from Cars, Catal. Today 163 (1) (2011) 33–41, https://doi.org/10.1016/j.cattod.2010.12.044.
[16] Y. Yazawa, H. Yoshida, N. Takagi, S. Komai, A. Satsuma, T. Hattori, Oxidation State of Palladium as a Factor Controlling Catalytic Activity of Pd/SiO2–Al2O3 in Propane Combustion, Appl. Catal. B Environ. 19 (3) (1998) 261–266, https://doi.org/10.1016/S0926-3373(98)00080-0.
[17] H. Yoshida, Y. Yazawa, T. Hattori, Effects of Support and Additive on Oxidation State and Activity of Pt Catalyst in Propane Combustion, Catal. Today 87 (1) (2003) 19–28, https://doi.org/10.1016/j.cattod.2003.10.001.
[18] P.M. Shah, A.N. Day, T.E. Davies, D.J. Morgan, S.H. Taylor, Mechanochemical Preparation of Ceria-Zirconia Catalysts for the Total Oxidation of Propane and Naphthalene Volatile Organic Compounds, Appl. Catal. B Environ. 253 (2019) 331–340, https://doi.org/10.1016/j.apcatb.2019.04.061.
[19] P.M. Shah, J.W.H. Burnett, D.J. Morgan, T.E. Davies, S.H. Taylor, Ceria–Zirconia Mixed Metal Oxides Prepared via Mechanochemical Grinding of Carbonates for the

Total Oxidation of Propane and Naphthalene, Catalysts 9 (5) (2019) 475, https://doi.org/10.3390/catal9050475.
[20] P.M. Shah, L.A. Bailey, D.J. Morgan, S.H. Taylor, The Effect of Metal Ratio and Precipitation Agent on Highly Active Iron-Manganese Mixed Metal Oxide Catalysts for Propane Total Oxidation, Catalysts 13 (5) (2023) 794, https://doi.org/10.3390/catal13050794.
[21] B. Solsona, T.E. Davies, T. Garcia, I. Vázquez, A. Dejoz, S.H. Taylor, Total Oxidation of Propane Using Nanocrystalline Cobalt Oxide and Supported Cobalt Oxide Catalysts, Appl. Catal. B Environ. 84 (1) (2008) 176–184, https://doi.org/10.1016/j.apcatb.2008.03.021.
[22] B. Solsona, T. García, R. Sanchis, M.D. Soriano, M. Moreno, E. Rodríguez-Castellón, S. Agouram, A. Dejoz, J.M. López Nieto, Total Oxidation of VOCs on Mesoporous Iron Oxide Catalysts: Soft Chemistry Route versus Hard Template Method, Chem. Eng. J. 290 (2016) 273–281, https://doi.org/10.1016/j.cej.2015.12.109.
[23] B. Solsona, R. Sanchis, A.M. Dejoz, T. García, L. Ruiz-Rodríguez, J.M. López Nieto, J.A. Cecilia, E. Rodríguez-Castellón, Total Oxidation of Propane Using CeO2 and CuO-CeO2 Catalysts Prepared Using Templates of Different Nature, Catalysts 7 (4) (2017) 96, https://doi.org/10.3390/catal7040096.
[24] G. Salek, P. Alphonse, P. Dufour, S. Guillemet-Fritsch, C. Tenailleau, Low-Temperature Carbon Monoxide and Propane Total Oxidation by Nanocrystalline Cobalt Oxides, Appl. Catal. B Environ. 147 (2014) 1–7, https://doi.org/10.1016/j.apcatb.2013.08.015.
[25] Z. Zhu, G. Lu, Z. Zhang, Y. Guo, Y. Guo, Y. Wang, Highly Active and Stable Co3O4/ZSM-5 Catalyst for Propane Oxidation: Effect of the Preparation Method, ACS Catal 3 (6) (2013) 1154–1164, https://doi.org/10.1021/cs400068v.
[26] Y. Xie, Y. Yu, X. Gong, Y. Guo, Y. Guo, Y. Wang, G. Lu, Effect of the Crystal Plane Figure on the Catalytic Performance of MnO2 for the Total Oxidation of Propane, CrystEngComm 17 (15) (2015) 3005–3014, https://doi.org/10.1039/C5CE00058K.
[27] T. García, J.M. López, B. Solsona, R. Sanchis, D.J. Willock, T.E. Davies, L. Lu, Q. He, C.J. Kiely, S.H. Taylor, The Key Role of Nanocasting in Gold-Based Fe2O3 Nanocasted Catalysts for Oxygen Activation at the Metal-Support Interface, ChemCatChem 11 (7) (2019) 1915–1927, https://doi.org/10.1002/cctc.201900210.
[28] P.M. Shah, L.A. Bailey, S.H. Taylor, The Influence of Cerium to Manganese Ratio and Preparation Method on the Activity of Ceria-Manganese Mixed Metal Oxide Catalysts for VOC Total Oxidation, Catalysts 13 (1) (2023) 114, https://doi.org/10.3390/catal13010114.
[29] J.A. Schwarz, C. Contescu, A. Contescu, Methods for Preparation of Catalytic Materials, Chem. Rev. 95 (3) (1995) 477–510, https://doi.org/10.1021/cr00035a002.
[30] X. Zhu, B. Cheng, J. Yu, W. Ho, Halogen Poisoning Effect of Pt-TiO2 for Formaldehyde Catalytic Oxidation Performance at Room Temperature, Appl. Surf. Sci. 364 (2016) 808–814, https://doi.org/10.1016/j.apsusc.2015.12.115.
[31] M.D. Argyle, C.H. Bartholomew, Heterogeneous Catalyst Deactivation and Regeneration: A Review, Catalysts 5 (1) (2015) 145–269, https://doi.org/10.3390/catal5010145.
[32] G. Chai, W. Zhang, Y. Guo, J.L. Valverde, A. Giroir-Fendler, A. The Influence of Residual Sodium on the Catalytic Oxidation of Propane and Toluene over Co3O4 Catalysts, Catalysts 10 (8) (2020) 867, https://doi.org/10.3390/catal10080867.
[33] T. García, B. Solsona, S.H. Taylor, Naphthalene Total Oxidation over Metal Oxide Catalysts, Appl. Catal. B Environ. 66 (1) (2006) 92–99, https://doi.org/10.1016/j.apcatb.2006.03.003.
[34] J. Ederer, M. Šťastný, M. Došek, J. Henych, P. Janoš, Mesoporous Cerium Oxide for Fast Degradation of Aryl Organophosphate Flame Retardant Triphenyl Phosphate, RSC Adv. 9 (55) (2019) 32058–32065, https://doi.org/10.1039/C9RA06575J.
[35] A.V. Radha, A. Navrotsky, Manganese Carbonate Formation from Amorphous and Nanocrystalline Precursors: Thermodynamics and Geochemical Relevance, Am. Mineral. 99 (5–6) (2014) 1063–1070, https://doi.org/10.2138/am.2014.4734.
[36] P. Venkataswamy, K.N. Rao, D. Jampaiah, B.M. Reddy, Nanostructured Manganese Doped Ceria Solid Solutions for CO Oxidation at Lower Temperatures, Appl. Catal. B Environ. 162 (2015) 122–132, https://doi.org/10.1016/j.apcatb.2014.06.038.
[37] H. Chen, A. Sayari, A. Adnot, F. Larachi, Composition–Activity Effects of Mn–Ce–O Composites on Phenol Catalytic Wet Oxidation, Appl. Catal. B Environ. 32 (3) (2001) 195–204, https://doi.org/10.1016/S0926-3373(01)00136-9.
[38] D. Sun, L. Peng, K. Cheng, Y. Zheng, S.P. Jiang, Comparative Study of Manganese Oxides with Different Oxidation States for Catalytic Carbonylation of N-Butylamine by CO2, J. CO2 Util. 68 (2023) 102382, https://doi.org/10.1016/j.jcou.2022.102382.
[39] Q. Wang, K.L. Yeung, M.A. Bañares, Ceria and Its Related Materials for VOC Catalytic Combustion: A Review, Catal. Today 356 (2020) 141–154, https://doi.org/10.1016/j.cattod.2019.05.016.
[40] L. Chen, J. Ding, J. Jia, R. Ran, C. Zhang, X. Song, Cobalt-Doped MnO2 Nanofibers for Enhanced Propane Oxidation, ACS Appl. Nano Mater. 2 (7) (2019) 4417–4426, https://doi.org/10.1021/acsanm.9b00818.
[41] T. Garcia, S. Agouram, J.F. Sánchez-Royo, R. Murillo, A.M. Mastral, A. Aranda, I. Vázquez, A. Dejoz, B. Solsona, Deep Oxidation of Volatile Organic Compounds Using Ordered Cobalt Oxides Prepared by a Nanocasting Route, Appl. Catal. A Gen. 386 (1) (2010) 16–27, https://doi.org/10.1016/j.apcata.2010.07.018.
[42] Y. Hammiche-Bellal, N. Zouaoui-Mahzoul, I. Lounas, A. Benadda, R. Benrabaa, A. Auroux, L. Meddour-Boukhobza, A. Djadoun, Cobalt and Cobalt-Iron Spinel Oxides as Bulk and Silica Supported Catalysts in the Ethanol Combustion Reaction, J. Mol. Catal. A Chem. 426 (2017) 97–106, https://doi.org/10.1016/j.molcata.2016.11.005.
[43] S. Dey, N.S. Mehta, Synthesis of CuMnOx Catalysts by Using Various Precipitants for Oxidation of Carbon Monoxide, Resources, Environ. Sustain. 4 (2021) 100025, https://doi.org/10.1016/j.resenv.2021.100025.
[44] B. Solsona, G.J. Hutchings, T. Garcia, S.H. Taylor, Improvement of the Catalytic Performance of CuMnOx Catalysts for CO Oxidation by the Addition of Au, New J. Chem. 28 (6) (2004) 708–711, https://doi.org/10.1039/B315391F.
[45] S. Dey, G.C. Dhal, D. Mohan, R. Prasad, Kinetics of Catalytic Oxidation of Carbon Monoxide over CuMnAgOx Catalyst, Mater. Discov. 8 (2017) 18–25, https://doi.org/10.1016/j.md.2017.09.001.
[46] W. Tang, J. Weng, X. Lu, L. Wen, A. Suburamanian, C.-Y. Nam, P.-X. Gao, Alkali-Metal Poisoning Effect of Total CO and Propane Oxidation over Co3O4 Nanocatalysts, Appl. Catal. B Environ. 256 (2019) 117859, https://doi.org/10.1016/j.apcatb.2019.117859.
[47] B. Tong, G. Meng, Z. Deng, M. Horprathum, A. Klamchuen, X. Fang, Surface Oxygen Vacancy Defect Engineering of P-CuAlO2 via Ar&H2 Plasma Treatment for Enhancing VOCs Sensing Performances, Chem. Comm. 55 (78) (2019) 11691–11694, https://doi.org/10.1039/C9CC05881H.
[48] B. Tong, G. Meng, Z. Deng, J. Gao, H. Liu, T. Dai, S. Wang, J. Shao, R. Tao, F. Kong, W. Tong, X. Luo, X. Fang, Sc-Doped NiO Nanoflowers Sensor with Rich Oxygen Vacancy Defects for Enhancing VOCs Sensing Performances, J. Alloys Compd. 851 (2021) 155760, https://doi.org/10.1016/j.jallcom.2020.155760.
[49] J. Kong, Z. Xiang, G. Li, T. An, Introduce Oxygen Vacancies into CeO2 Catalyst for Enhanced Coke Resistance during Photothermocatalytic Oxidation of Typical VOCs, Appl. Catal. B Environ. 269 (2020) 118755, https://doi.org/10.1016/j.apcatb.2020.118755.
[50] P. Wang, X. Ma, X. Hao, B. Tang, A. Abudula, G. Guan, Oxygen Vacancy Defect Engineering to Promote Catalytic Activity toward the Oxidation of VOCs: A Critical Review, Catal. Rev. 66 (2) (2024) 586–639, https://doi.org/10.1080/01614940.2022.2078555.
[51] L. Chen, Y. Liu, X. Fang, Y. Cheng, Simple Strategy for the Construction of Oxygen Vacancies on α-MnO2 Catalyst to Improve Toluene Catalytic Oxidation, J. Hazard. Mater. 409 (2021) 125020, https://doi.org/10.1016/j.jhazmat.2020.125020.
[52] Y. Zheng, K. Fu, Z. Yu, Y. Su, R. Han, Q. Liu, Oxygen Vacancies in a Catalyst for VOCs Oxidation: Synthesis, Characterization, and Catalytic Effects, J. Mater. Chem. A 10 (27) (2022) 14171–14186, https://doi.org/10.1039/D2TA03180A.